frontiers | Frontiers in Physics

TYPE Review
PUBLISHED 22 November 2024
DOI 10.3389/fphy.2024.1447696

OPEN ACCESS

EDITED BY
Riccardo Meucci,
National Research Council (CNR), Italy

REVIEWED BY
Liviu Goras,
Gheorghe Asachi Technical University of Iași, Romania
Kais A. Al Naimee,
University of Baghdad, Iraq

*CORRESPONDENCE
Wenxiang Liu,
liuwenxiang08@nudt.edu.cn

RECEIVED 12 June 2024
ACCEPTED 30 October 2024
PUBLISHED 22 November 2024

CITATION
Song Y, Wang H, Liu W, Xiao W, Ye X and Sun G (2024) A review on the mechanism of high repetition rate pulse interference on the RF front-end of GNSS receivers.
Front. Phys. 12:1447696.
doi: 10.3389/fphy.2024.1447696

A review on the mechanism of high repetition rate pulse interference on the RF front-end of GNSS receivers

Yili Song[1,2], Huilin Wang[3], Wenxiang Liu[1,2]*, Wei Xiao[1,2], XiaoZhou Ye[1,2] and Guangfu Sun[1,2]

[1]College of Electronic Science and Technology, National University of Defense Technology, Changsha, China, [2]Key Laboratory of Satellite Navigation Technology, Changsha, China, [3]China Satellite Navigation Office, Beijing, China

With the rapid advancement of pulse technology, given the extraordinarily high repetition frequency of high-repetition pulse interference, with pulse widths typically ranging from a few nanoseconds to several hundred nanoseconds, it possesses ultra-wideband characteristics, research on how to avoid spectral conflict and malicious interference between these pulse signals and navigation receiver systems has emerged as a pressing and popular issue. This paper introduces the mathematical model of high repetition pulse interference signals. Following this, the paper summarizes and analyses the transient response, nonlinear distortion, and linear distortion that accompany signal processing at the Radio Frequency (RF) front end of the receiver. It concludes that the main source of interference in the limiter's transient response is peak leakage, the primary factor in low noise amplifier's (LNA) interference is third-order intermodulation distortion, and filter interference is due to the interlaced response from adjacent pulses. Lastly, the current research progress on the mechanism of high repeti-tion pulse interference with navigation receivers is reviewed, providing reference for future study.

KEYWORDS

high-repetition-rate interference, mechanism analysis, nonlinear distortion, transient response, interlaced response

1 Introduction

Currently, the interference to navigation receivers can be classified into two categories: jamming and spoofing [1]. Due to the low power of satellite signals at the ground receiver, typically around −160 dBW, they are vulnerable to interference [2]. Jamming interference suppresses receiver performance by utilizing high-power noise signals. With the advancement of pulse technology, high-repetition-rate pulse signals have gained a unique advantage in the field of receiver interference due to their faster rise/fall time, narrower pulse width, and higher repetition rate. Consequently, research on using high-repetition-rate pulse signals to counter receiver interference has emerged. [3] focuses on the suppression of radar receivers using high-repetition-rate pulses, while [4] investigates the dependency of the interference effect on pulse parameters and pro-poses methods for optimal design of interference pulse width and repetition rate. [5] explores the interference mech-anism of repetition rate pulses on the RF front

end of passive guidance heads, and [6] studies the effects of different pulse parameters on the receiver.

However, most of the existing research on navigation receivers mainly revolves around the relationship between pulse pa-rameters and interference effects, lacking a thorough analysis of the interference mechanism on the RF front end of navigation receivers. To address this gap, this paper summarizes the transient response distortion and nonlinear distortion of a series of RF front-end components, including limiters, low-noise amplifiers, filters, and Automatic Gain Control (AGC). It provides a com-prehensive understanding of the interference mechanism of high-repetition-rate pulses on the receiver front end.

This article is organized as follows. Section 2 delves into the intricacies of high-repetition-rate pulse signal models, elaborating on the signal characteristics in both the time and frequency domains. Section 3 synthesizes the primary influences im-pacting the receiver's RF front-end, providing a comprehensive review of the interference mechanisms. This includes an analy-sis and discussion of transient response distortions, notably the spike leakage and recovery time power attenuation generated by limiters, as well as the transient response distortions of AGC. Regarding nonlinear distortions, the focus is on summarizing and analyzing third-order intermodulation distortions caused by LNA and nonlinear distortions introduced by mixers, with a com-parative analysis at both the signal and mechanism levels. The response distortions associated with filters are explored through the examination of distortions brought about by front-end devices and their varied impacts. Section 4 consolidates the core con-tributions of this work, outlines potential future directions for this field, and offers fresh perspectives on the design of RF front-ends for receivers and anti-interference strategies. Through a dialectical analysis and comparison of existing mechanism re-search findings, this article elucidates the current understanding of high-repetition-rate pulse interference on Global Navigation Satellite System (GNSS) receiver front-ends. It discusses future trends and research directions in analyzing the mechanisms of interference, providing valuable insights for the development of effective mitigation strategies to protect navigation receivers against high-repetition-rate pulse interference.

2 Characteristics of high-repetition-rate pulsed signals

High-repetition-rate pulse signals are characterized by their nanosecond-level pulse width, extremely high repetition frequency, and wide frequency spectrum [7]. Denoted by A as the pulse amplitude, N as the number of pulses, T_r as the repetition period, τ as the pulse width, these signals can be mathematically expressed as Equation 1:

$$j(t) = A \cdot \sum_{n=0}^{N-1} rect\left(\frac{t - nT_r}{\tau}\right) \tag{1}$$

where $rect(\cdot)$ is the rectangular function.

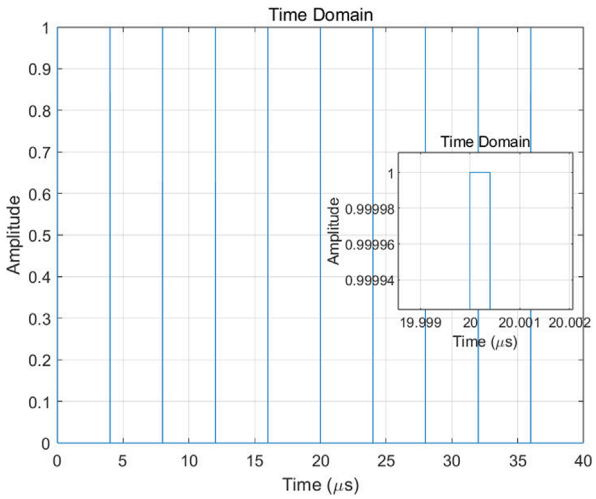

FIGURE 1
Waveform of high-repetition-rate frequency pulse. The time domain result of the signal.

The Fourier transform of the time-domain signal yields the frequency-domain expression Equation 2 for the high-repetition-rate pulse as:

$$J(f) = A \cdot \tau \cdot \sin c(\tau \cdot f) \frac{\sin \pi fNT}{\sin \pi fT} e^{-j\pi f(N-1)T} \tag{2}$$

where Sinc(·) denotes the Sinc function, which arises in the context of the Fourier transform of a rectangular pulse signal. The Sinc function is defined as Sinc(x) = sin(πx)/(πx), representing the spectral distribution of a rectangular pulse in the frequency domain.

The time domain result of the signal is shown in Figure 1. The signal parameters are as follows: the pulse width is 1 nanosecond, the repetition period is 4 microseconds, the sampling frequency is 10 GHz, and the number of pulses is 10. Given the very narrow pulse width, the vertical lines in Figure 1 represent the pulses. The rise and fall times of the pulses are assumed to be zero, indicating instantaneous rise and fall.

By performing Fourier transform on the time domain result, the frequency domain result is plotted as shown in Figure 2.

As depicted in Figures 1, 2, the pulse parameters include an amplitude of 1, a pulse width of 1 nanosecond (ns), and a repetition period of 4 microseconds (us), resulting in a remarkably high repetition rate in the temporal domain and endowing the frequency domain with ultra-wideband characteristics. The spacing between adjacent spectral lines is equal to the pulse repetition frequency. The spectral waveform envelope conforms to a Sinc(·) function and occupies an extensively broad spectral range. The wide bandwidth of the high-repetition-rate pulse interference signal allows it to overlap with the operational frequency bands of GNSS receivers, potentially causing internal interference within the receiver's RF front-end components.

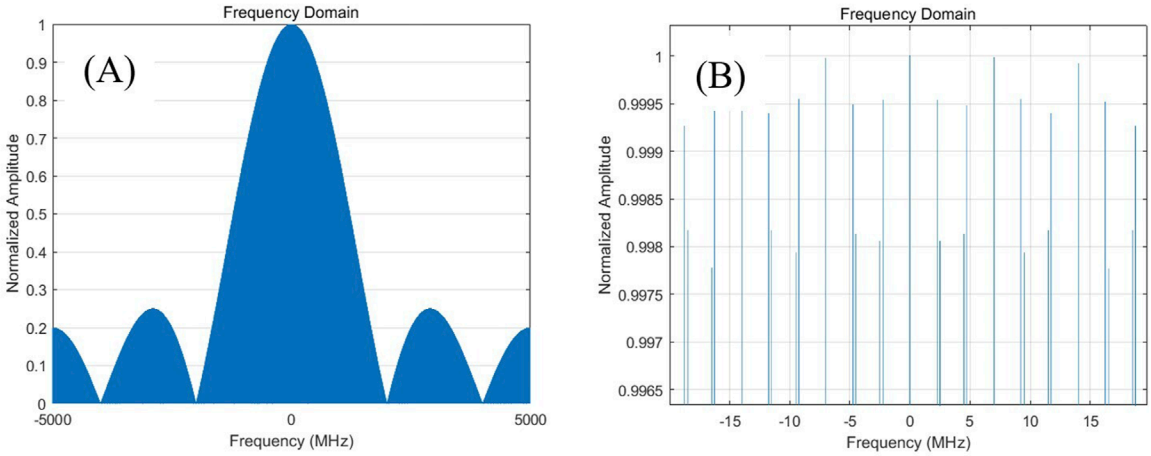

FIGURE 2
Depicts the frequency domain plot of the high-repetition-rate pulse signal. **(A)** illustrates the frequency domain representation of the high-repetitionrate ultra-wideband pulse, while **(B)** shows an enlarged view of the frequency domain response of the high-repetition-rate ultra-wideband pulse near 0 MHz. illustrates the frequency domain response of the high-repetition-rate ultra-wideband pulse.

3 Summary of mechanisms for high repetition rate pulse interference

When high-repetition-rate pulse interference is applied to navigation receivers, the leading and trailing edges as well as the duration of the interference pulses are extremely short. Such interference pulses can cause significant transient responses in the receiver front-end [8–10]. Transient response is the process by which a system arrives at a steady state from an initial state when subjected to a typical signal input, and is usually expressed in the time domain as the response time of the system. This type of transient response may manifest as rapid changes, oscillations, or distortions in the output signal of the analog front-end.

Due to the non-ideal nature of actual front-end components in receivers [11–14], performing filtering, amplification, and other operations on the received signals can result in the generation of nonlinear distortion due to the nonlinear characteristics of these practical components. The increase in distortion product power not only reduces the signal-to-noise ratio of the front-end output but also renders the digital signals produced by Analog-to-Digital Converter (ADC) conversion unable to carry valid navigation information. Consequently, this factor affects the subsequent processing of the signals.

3.1 Receiver front-end transient response distortion summary

3.1.1 Limiter transient response distortion

The interfering signal received by the antenna will first be responded to by the limiter and subsequently fed to the next level of RF devices for processing. Since the signal is fed into the RF filter for processing after the limiter, the front and back edges of the signal pulse after being subjected to the band-pass filter become slow, so the transient response of the back-stage analog device to the high-repetition-rate pulse will no longer be significant [15].

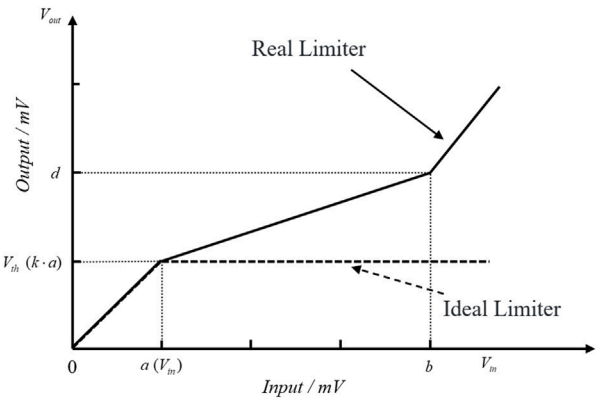

FIGURE 3
limiter operating characteristic curve. The operating characteristic curve of the limiter.

The operating characteristic curve of the limiter is shown in Figure 3.

The operational characteristics of the limiter are illustrated in Figure 3. In the ideal case, when the amplitude of the input signal has not reached the threshold, the amplitude of the output signal increases linearly with the amplitude of the input signal. After reaching the threshold, the amplitude of the output signal will be clipped to this threshold. In the real case, as the input power increases, the output signal amplitude of the limiter undergoes a proportional increase at low input power levels. When the input signal exceeds the threshold level, the limiter begins to operate, resulting in a slower rate of increase in output signal amplitude. If the input power continues to increase, the internal PIN diode of the limiter operates in the saturation region, causing the limiter to become ineffective until the device is burnt out. The

TABLE 1 Output signal power attenuation percentage %.

tx (ns)	Pulse repetition frequency (kHz)				
	50 kHz	100 kHz	150 kHz	200 kHz	250 kHz
50 ns	0.12%	0.25%	0.37%	0.50%	0.62%
100 ns	0.25%	0.50%	0.75%	1.00%	1.25%
150 ns	0.37%	0.75%	1.12%	1.50%	1.87%

[a]Table 1 data summarized from simulation experiments conducted by Haonan and colleagues [5]. Output signal power attenuation law. Data presented in Table 1 illustrate that as the response time of the limiter, (tx), increases from 50 nanoseconds (ns) to 200 nanoseconds, there is a gradual enhancement in the attenuation of the output signal power at consistent interference pulse frequencies.

primary reasons for damaging the operational characteristics of the PIN limiter are attributed to peak leakage and recovery time effects.

Extensive research has indicated that in practical experiments, the transient response of limiters, including peak leakage, flat leakage, and recovery time, plays a significant role in causing damage to both the limiters themselves and subsequent power-sensitive components [4, 16, 17].

Peak leakage refers to the weak limiting effect of the diode on high-power microwave RF signals when the diode is in a high impedance state. Therefore, for highly repetitive interference with extremely narrow pulse widths, if the rise time of the pulse is shorter than the response time of the limiter, the peak leakage effect will result in the limiter missing high-amplitude interference pulses, allowing them to enter the subsequent system. As discussed earlier, the rise time plays a critical role in determining how the limiter responds to transient signals, and failure to account for this can lead to significant leakage of high-amplitude pulses.

Recovery time refers to the period during which the limiter's isolation remains significant while the input signal power rapidly decreases due to the trailing edge of a pulse signal. This time interval, from the termination of the input pulse to when the limiter's loss exceeds the insertion loss by 3 dB, is considered the recovery time of the limiter.

- Recovery Time: When the recovery time of the limiter is relatively small, its impact on the received signal in the subsequent signal processing system is minor and can be approximately disregarded [4, 18].
- Peak Leakage: When the repetition frequency of the interfering pulse is 50 MHz, the interference signal overlaps front and back edges after filtering due to the pulse repetition period being shorter than the filter response time, completely suppressing the radar signal post-detection. Whereas, when the interference pulse repetition period is longer than the filter response time, adjacent pulses do not overlap after passing through the filter. However, as adjacent frequency components primarily mask noise amplitude modulation interference, the effective signal is equally suppressed when the interference power is sufficiently large [5, 18, 19].

The output signal power law shown in Table 1 below can be derived by summarising the simulation experiments of Nan Hao et al [5].

Data presented in Table 1 illustrate that as the response time of the limiter (tx), increases from 50 nanoseconds (ns) to 200 nanoseconds, there is a gradual enhancement in the attenuation of the output signal power at consistent interference pulse frequencies. Furthermore, it is observed that higher interference pulse frequencies correlate with greater reductions in output signal power, albeit the maximal decrease remains below 2%. These experimental findings corroborate the theoretical analysis, asserting that the recovery time serves as a secondary influencing factor.

Analysis for the transient response interference mechanism of high-repetition-rate pulses on limiters can be summarized as follows:

- Within the prescribed detection parameters of a receiver, it has been observed that peak leakage originating from the limiter engenders an escalation in the input signal power exposed to the LNA. This relationship dictates that the power spectrum of intermodulation distortion inherent to the LNA exhibits a direct proportionality to the magnitudes of the input signal power. Consequently, such escalation attributable to peak leakage unequivocally intensifies the non-linear distortion experienced by the ensuing analog components. The phenomena underscore the pernicious effect of peak leakage on the linear behavior of analog signal processing, necessitating a stringent control mechanism to circumvent the exacerbation of non-linear distortion [5, 11, 20].
- Conversely, in scenarios where the received signal power eclipses the designed dynamic range of the receiver, an ensuing peak leakage incident within the limiter precipitates excess signal power influx into the downstream system, leading to a surpassing of the subsequent analog components' dynamic range. Manifestations of this signal excess are saturation, overload, or an involuntary reduction in gain at the analog front-end of the receiver. This pervasive chain reaction signifies a critical operational failure, triggering an array of deleterious effects that undermine the receiver's analog front-end performance. Under such conditions, the analog front-end is compelled to operate outside its nominal range, incurring signal integrity degradation and diminishing the overall system efficacy. Therefore, it is imperative that receivers are designed or equipped with adaptive features to mitigate such instances of peak leakage that potentially imperil the functional stability of analog components [21, 22].

In order to further investigate the impact of pulse repetition frequency (PRF) on GPS receivers, Morton, Huang Bangju, and others [23, 24] conducted experiments by generating high-repetition-rate pulses to interfere with GPS receivers. It was observed that as the PRF of the pulses increased, the signal acquisition rate of the GPS receivers decreased; notably, this decline became significantly more pronounced when the repetition frequency approached the data transmission rate of communication signals.

In the context of practical application testing, Zhao Tongcheng et al. [25] used drones equipped with GPS receivers as experimental subjects to test four distinct high-repetition-rate pulses combinations: Mode A (a single 200 kHz), Mode B (one 200 kHz and one 300 kHz), Mode C (two 200 kHz), and Mode D (two 200 kHz and one 300 kHz). The experiment demonstrated significant interference of high-repetition-rate pulses on drone GPS systems. Under testing conditions, drones exhibited maximum loss of control distances reaching hundreds of meters, with complete signal interruption from ground-based controllers, leading to a range of hazardous behaviors including acceleration, hovering, or deviating from the flight path. This experiment also corroborated the theoretical analysis concerning the impact of pulse repetition frequency on receiver interference.

The interference theoretical analysis on the receiver's front-end RF components, built upon previous studies focused on the singular increase in pulse repetition frequency's impact on receiver interference, has been further developed by researchers such as YongX, HuangX, etc. [21, 26]. They employed a pulse model for modeling and analyzing the interference, primarily examining the interference outcomes related to the relationship between pulse repetition frequency and receiver operational bandwidth. The effects of repetition frequency interference on the Bit Error Rate (BER) of GPS receivers were theoretically analyzed [27], as well as the impact of high-repetition-rate pulses on the GPS signal rate. The results indicated that at high signal strength states, the GPS signal intensity required to maintain a fixed bit error rate and data rate is inversely proportional to the Pulse Repetition Frequency.

1. It is well-documented in the literature [21, 28] that the interference effect of high-repetition-rate pulses on Global Positioning System operations is contingent upon the spectral alignment of the high-repetition-rate pulse signals components with the GPS frequency band. It has been determined that when the integer multiples of the pulse repetition frequency of the signal do not coincide with the GPS operational bandwidth, and in the absence of strong, amplitude-oriented single pulses in proximity to the GPS center frequency, the resultant interference exerted upon the GPS receiver is markedly attenuated. Conversely, it has been found that when the aforementioned integer multiples of the PRF align with the GPS signal's center frequency, the interference effect is significantly magnified, exerting the maximum impact on the GPS receiver's signal integrity.
2. Investigations into the effects of repeat pulse signals within the functional bandwidth of GPS receivers have revealed [26, 29] an inverse relationship between the pulse repetition frequency and the consequential interference with GPS signals. Specifically, a lower PRF correlates with a reduction in the average power of the high-repetition-rate pulses. Consequently, this diminished power of the repeat pulse signal is associated with a less intrusive influence on the GPS signal. This finding underscores the criticality of PRF selection in the design and operation of systems where the potential for high-repetition-rate pulses interference with GPS signals must be judiciously mitigated to preserve navigational accuracy and reliability. The data indicates the substantial role that PRF plays in determining the level of cross-signal interference and highlights the necessity for strategic management of pulse repetition parameters in high-repetition-rate pulses systems to avert detrimental impacts on GPS functionality.

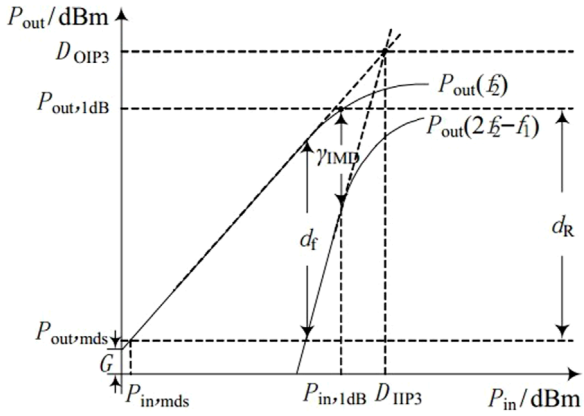

FIGURE 4
Receiver front-end processing. Pulses with high repetition frequencies induce nonlinear responses in the functional modules of a receiver.

In summary, the repetition frequency of high-repetition-rate pulse has a significant impact on receivers. Interference intensifies as the pulse frequency increases, with the signal recognition rate of receivers experiencing a substantial decline when the frequency approaches the actual communication frequency of high-repetition-rate pulses. Interference becomes particularly pronounced and challenging to mitigate when the integer multiples of the pulse frequency fall within the operational bandwidth of the receiver, complicating the removal of the pulse's nonlinear distortion during subsequent processing.

3.1.2 AGC transient response distortion

Pulses with high repetition frequencies induce nonlinear responses in the functional modules of a receiver. These responses transform nanosecond-level signals into secondary interference signals, with the durations extending to several hundred nano-seconds, as illustrated in Figure 4 [30, 31]. This process results in the perturbation of the AGC circuitry by the afo rementioned secondary interference signals. Subsequently, this perturbation leads to the generation of aberrant AGC control voltages that attenuate the gain within the receiving system. As a consequence, the amplification of normal signals is impeded, which dimin-ishes the signal-to-noise ratio (SNR) and escalates the BER. Upon surpassing the system's threshold for gain reduction, the possibility of temporary communication disruption emerges.

TABLE 2 Device response latency.

Receiver front-end device (RFP)	Latency
connection with high-ranking officials	<10 ns
mixer	Tens of ns
filters	Tens of ns
low-noise amplifier	Hundreds of ns ~ us

[a]Table 2 data summarized from experimental findings by ZhangY et al. The prolonged durations of interference signals in different devices were studied.

After passing through the antenna, limiter, filter, LNA, and mixer, are converted into secondary interference signals with significantly prolonged durations—ranging from several hundred nanoseconds to even a few microseconds. Then, the AGC circuit is impacted by these secondary interference signals, and the AGC control voltage becomes abnormal, causing a decline in receiver system gain. This insufficient amplification of normal signals can lead to a temporary interruption in communication. Furthermore, when the repetition frequency is sufficiently high, the interruption of communication may persist.

Further research by ZhangY et al. [32] revealed that the output duration of critical components affected by high repetition frequency electromagnetic pulses is not related to the repetition frequency, but rather to the amplitude of the interference signal. Since the AGC circuit will gradually recover after interference from a single electromagnetic pulse, such disturbances are transient.

Moreover, through experimental measurements and simulation analysis, the prolonged durations of interference signals in different devices were studied, as indicated in Table 2.

Summary of the reasons for the extended duration of interference signals is as follows:

- The response exhibited by antennas and filters to electromagnetic pulses of high repetition frequency is characterized by linearity. In contrast, Low Noise Amplifiers (LNAs) and limiters manifest a nonlinear response, with the capability of all such responses to prolong the signal duration. Notably, the duration extension attributed to the LNA is the most significant, potentially extending to hundreds of nanoseconds, or in certain instances, even a few microseconds. This phenomenon is primarily related to the bandwidth limitations of the LNA, which can cause a narrowing of the spectral content and, consequently, an elongation of the waveform in the time domain.
- Passive devices, operating within a narrower frequency band relative to the broad spectrum of high-repetition-rate pulses, induce a spectral narrowing when these pulses pass through them. This spectral constriction is correspondingly manifested as an elongation of the waveform in the time domain. Similarly, the bandwidth limitations of active devices like LNAs can also lead to an extension of signal duration due to the spectral narrowing effect.
- The extension of output duration in active devices can be attributed predominantly to the impact exerted by high-repetition-rate pulses on the peripheral circuits, which is further influenced by the bandwidth limitations of these devices. These circuits, integral to the device chips, contribute to the noted extension effects primarily through spectral narrowing and subsequent waveform elongation.

3.2 Low noise amplifier and mixer nonlinear distortion

The functions of the LNA and the mixer include enhancing and amplifying weak signals output by the limiter, thus facilitating the further processing of signals by subsequent components [33]. In practical operation, the LNA not only amplifies the input signal linearly, but also generates certain harmonic and intermodulation components, which leads to nonlinear distortion [34]. Given the numerous frequency components of high-repetition-rate pulses, various nonlinear distortion products are inevitably generated at the receiver's frontend. Among these, the third-order intermodulation component, due to its strong amplitude among odd-order intermodulation components and frequency closest to the source signal, is particularly difficult to eliminate through filtering. Therefore, it possesses a high likelihood of causing severe interference with the signal processing of navigation receivers [35].

The primary sources of nonlinear distortion at the front end of the receiver originate from the LNA and the mixer. As indicated by the operational range of the linear devices shown in Figure 5, an abrupt transition occurs as the Low Noise Amplifier (LNA) moves from the linear amplification region to the nonlinear distortion region. In the linear region, the amplifier's output power increases proportionally with the input power, and the third-order intermodulation product increases at a rate three times that of the output signal's power. However, once the input power exceeds the amplifier's 1 dB compression point, the amplifier enters a nonlinear state, leading to a sharp reduction in gain. This transition marks the onset of significant nonlinear distortion, where the amplifier's output no longer follows the input signal proportionally, resulting in the observed abrupt change [11].

The graphs in Figure 5 also provide insights into the behavior of nonlinear devices. Specifically, when the input power exceeds the 1 dB compression point, the LNA and mixer enter a nonlinear state, resulting in significant third-order intermodulation distortion (IMD3). This nonlinearity is illustrated by the departure from proportional output power increase, as shown in the figure. The analysis of these graphs aids in understanding the nonlinear response and helps in designing measures to mitigate distortion effects in nonlinear devices.

From Figure 5, let P_{in} and P_{out} represent the input power and output power of the system, respectively. Define $P_{\text{in,mds}}$ as the minimum power of the input signal, $P_{out,mds}$ as the minimum power of the output signal, f_1 as the frequency of the useful signal, and f_2 as the frequency of the interference signal. Here, $P_{out}(f_2)$ denotes the signal output power, $P_{out}(2f_2 - f_1)$ refers to the output power of the third-order product of harmonics and signal, G represents the device's amplification gain, and d_f signifies the undistorted dynamic range. Additionally, d_R is defined as the dynamic range, $P_{in,1dB}$ as the

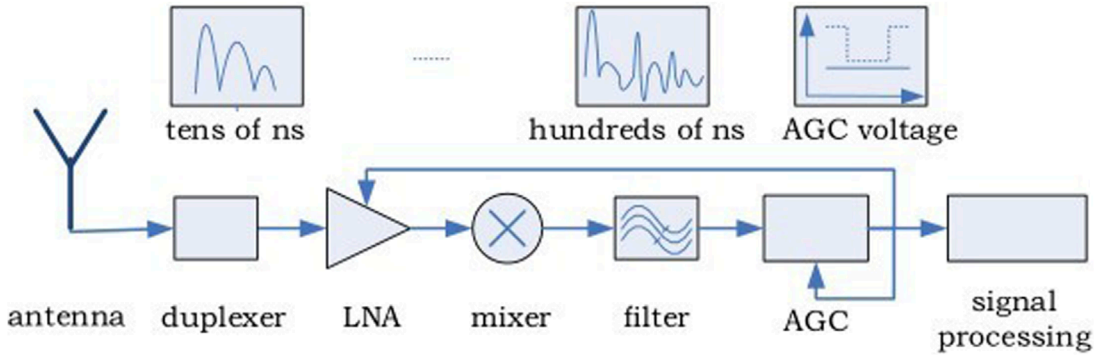

FIGURE 5
Third-order cross-modulation distortion curves for linear devices. The primary sources of nonlinear distortion at the front end of the receiver originate from the LNA and the mixer. As can be inferred from the operational range of the linear devices shown in Figure 5, when the input power exceeds the 1 dB compression point of the device, the amplifier enters a nonlinear state.

input 1 dB compression point (measured in dBm), and $P_{out,1dB}$ as the output 1 dB compression point, the following formula Equation 3 for third-order intermodulation distortion can be derived:

$$\begin{cases} P_{out} = P_{\text{int}} + G \\ P_{out,1dB} = P_{\text{int},1dB} + G \\ \gamma_{IMD} = P_{out}(f_2) - P_{out}(2f_2 - f_1) \\ D_{OIP3} = D_{IIP3} + G \approx P_{out,1dB} + 10 \\ D_{IMD3} = 3P_{out} - 2D_{OIP3} \end{cases} \tag{3}$$

where, γ_{IMD} is the intermodulation distortion coefficient; D_{IIP3} and D_{OIP3} are the input and output third-order intercept points, correspondingly; and D_{IMD3} denotes the third-order intermodulation distortion power.

The third order intermodulation distortion power D_{IMD3} can be expressed as:

$$D_{IMD3} = 3P_{in} + G - 2D_{IIP3} \tag{4}$$

$$D_{IMD3} = 3P_{in} - 2P_{in,1dB} + G - 20 \tag{5}$$

If the input third-order intercept point (IIP3) of a linear device is known, then Equation 4 should be employed for calculation; otherwise, Equation 5 is utilized. Equation 4 delineates the relationship between the input power, the gain of the analog device, the input third-order intercept point, and the intermodulation distortion, which is typically used for computing the non-linear distortion of a LNA. On the other hand, Equation 5 reflects the correlation among input power, the 1 dB compression point at the input, the gain of the analog device, and the intermodulation distortion, and it is generally applied to calculate the non-linear distortion of mixers.

- Third-order intermodulation distortion in the LNA: Padgett, Wang Tonggang, and others [22, 35] conducted experimental analyses of the nonlinear distortion of the LNA and concluded that high-repetition frequency ultra-wideband pulses after passing through the LNA produce third-order intermodulation distortion frequencies that fall near the working frequency range of the receiver and can enter the subsequent stages of the receiver. When the power of the transmitted interference signal is high, the power of the resulting third-order intermodulation distortion is also correspondingly high. The superimposition of the third-order intermodulation distortion components with high-repetition frequency ultra-wideband pulses can cause significant impact on the subsequent signal processing stages.
- Mixer nonlinear distortion: Wang Tonggang and colleagues [35] conducted tests to assess the impact of frontend nonlinear distortion in receivers, and discussed whether different linear devices would exhibit nonlinear distortion under various power levels of the interfering signal through theoretical deductions. The experimental results are demonstrated in the following Table 3.

An analysis of the data in Table 3 indicates the impacts of nonlinear distortion in the mixer, wherein the 1 dB compression point of the mixer input is the smallest, tending to induce nonlinear distortion. If the interference power exceeds −20 dBm, the mixer generates an increased ratio of nonlinear distortion as the interference power increases. When the interference power is low, no nonlinear distortion arises in the linear components. The frequency conversion loss of the mixer is considered to be minimally affected by the high-repetition-rate pulses. However, the LNA generates nonlinear distortion when the interference power exceeds 2 dBm.

From the perspective of power spectral density, the degree of degradation in the carrier-to-noise ratio (C/N0) of the GPS receiver was theoretically derived.

- Swami, Xu Jie, and others [10, 36, 37] simulated and analyzed to derive the curve of the relationship between GPS receiver C/N0 and interfering distance. By examining the equivalent C/N0 of GPS receivers under interference, XinHuang [26] theoretically calculated the lowest interference level of the interfering signal to be −130 dBW, which seriously interferes with the loop tracking process in the receiver, leading to positioning loss. Simultaneously, when the ratio of interference signal power to useful signal power (Jamming to signal ratio) is approximately 30 dB, the system's BER approaches 0.5. This

TABLE 3 Distortion power (dBm) of first-stage mixer.

TV or radio receiver interference power(dBm)	Mixer Distortion power(dBm)	Reaching the next level Mixer Power(dBm)	First-stage mixer Specific gravity of distortion power(dBm)
−22	−24	−19.87	0.39
−21	−21	−17.99	0.50
−20	−18	−15.88	0.61

[a]Table 3 data summarized from experimental findings by Wang Tonggang et al [29]. Nonlinear distortion influence law of mixers. Wherein the 1 dB compression point of the mixer input is the smallest, tending to induce nonlinear distortion.

significantly lowers system performance and prevents correct demodulation of navigation message data.

- Anderson, TingtingLu, et al [29, 38, 39] used BDS receivers, with the second derivative of a Gaussian pulse as the actual interfering signal, to study the effect of the interfering signal's radiating power on the BeiDou signal. The experiment found that the power spectral density of a high-repetition-rate pulses with an equivalent isotropic radiated power (ERIP) of −53.3 dBm covered the entire bandwidth (1500–1600 MHz) of the BeiDou B1 signal. Although the regulation from the Ministry of Industry and Information Technology suggests minimal impact with an ERIP of −90 dBm, the proximity of the center frequency to the BeiDou signal cannot be ignored. Superimposing the BeiDou signal with the ultra-wideband signal could drown out the former.
- When considering factors such as multipath fading and Gaussian noise in the receiver, ZhangXiangyu and others [29] found through experiments that as the power of the ultra-wideband signal increases, the performance of the direct-sequence spread spectrum (DS-SS) rapidly declines due to severe noise interference. However, if the noise and high-repetition-rate pulse signals high-repetition-rate pulses SS performance will not be noticeably affected.

The research explores interference effects on GPS and BeiDou signals. Swami et al. establish the C/N0 vs. interfering distance relationship for GPS receivers, with critical interference noted at −130 dBW, leading to positioning loss. A 30 dB jamming to signal ratio results in a BER of 0.5, degrading system performance. Anderson, TingtingLu, et al. demonstrate that high ERIP (−53.3 dBm) pulses can overshadow BeiDou signals, despite regulatory thresholds at −90 dBm. ZhangXiangyu et al. find that escalating ultra-wideband signal power compromises DS-SS performance due to noise interference, while noise and high-repetition-rate pulse signals have minimal impact. These findings underscore the importance of mitigating interference for satellite navigation system reliability.

Through mechanism analysis, the conditions under which high-repetition-rate pulses interfere with GPS receivers were derived, as indicated by Equation 6.

$$10\lg\left\{\frac{\pi e\left(Af_{prf}\right)^2}{8R}\sum_{n=-a/f_{prf}}^{b/f_{prf}}\left[\tau^2 n f_{prf} e^{-\frac{\pi\tau^2}{4}\left(nf_{prf}\right)^2}\right]^2\right\}\geq J \tag{6}$$

Where, J denotes the receiver interference tolerance, f_{prf} denotes the repetition frequency, and τ denotes the pulse width.

Based on Equation 6, the critical interference condition for a GPS receiver to lose lock can be further deduced.

$$10\lg\left[B_1 {B_2}^2 B_3\right] = J \tag{7}$$

$$B_1 = \frac{\pi e}{8R} \tag{8}$$

$$B_2 = Af_{prf} \tag{9}$$

$$B_3 = \sum_{n=-a/f_{prf}}^{b/f_{prf}}\left[\tau^2 n f_{prf} e^{-\frac{\pi\tau^2}{4}\left(nf_{prf}\right)^2}\right]^2 \tag{10}$$

As indicated by Equations 7–10, when the pulse width decreases, the main frequency range of the pulse broadens and its central frequency shifts towards higher frequencies. Consequently, within the operational frequency band of the GPS receiver, the power of the pulse initially increases and then decreases. Accordingly, the amplitude of the pulse corresponding to the moment when the receiver loses lock first diminishes and subsequently augments.

In 2014, Zhang Zhixiang et al. [6] established a simulation analysis experiment for the receiver using Matlab/Simulink software to test the pulse amplitude required to cause receiver unlock at different pulse widths. They found that when the pulse width was approximately 0.29 microseconds and the center frequency was approximately 1.1 GHz, the pulse amplitude corresponding to receiver unlock was minimal, indicating the strongest interference effect of high-repetition-rate pulses on the receiver.

In 2021, Wang Tonggang et al. [35], building upon the foundational research of Zhang Zhixiang, Liu Ruihua [6, 40–42] on high-repetition-rate pulses causing receiver unlock, further examined the mechanism of nonlinear distortion at the front end of the receiver, focusing on the RF front-end analog section before the L1 signal is down converted to 4.309 MHz through three stages of mixing.

Their research showed that as the pulse width increased, the interfering power entering the receiver gradually rose. When surpassing the 1 dB compression point of linear devices' input, diverse linear devices sequentially experienced nonlinear distortion, causing a sudden change in the signal-to-interference-plus-noise ratio (SINR). The front-end SINR test results for its receivers are summarized in Table 4 below:

TABLE 4 Summary of receiver simulation test pulse width interference data.

Interference pulsewidth/us	Disregarding non-linear distortion		Consider non-linear distortion		Signal-to-noise ratio Difference/dB
	Interference power/dBm	Signal-to-noise ratio /dB	Interference power/dBm	Signal-to-noise ratio /dB	
0.40	−22.66	−86.34	−22.66	−86.34	0
0.45	−22.21	−86.79	−22.21	−86.79	0
0.50	−21.79	−87.21	−19.50	−89.50	2.29
0.55	−21.44	−87.56	−18.84	−90.16	2.60
0.60	−21.10	−87.90	−18.20	−90.80	2.91
0.65	−20.80	−88.20	−17.58	−91.42	3.22
0.70	−20.51	−88.49	−16.98	−92.02	3.53
0.75	−20.24	−88.76	−16.40	−92.60	3.84
0.80	−19.99	−89.01	4.79	−113.79	24.78

[a]Table 4 data summarized from experimental findings by Zhang Zhixiang, Liu Ruihua et al [10, 36]. Summarize the effect of different pulse width interference on the receiver's interference power by analyzing whether or not to consider nonlinear distortion.

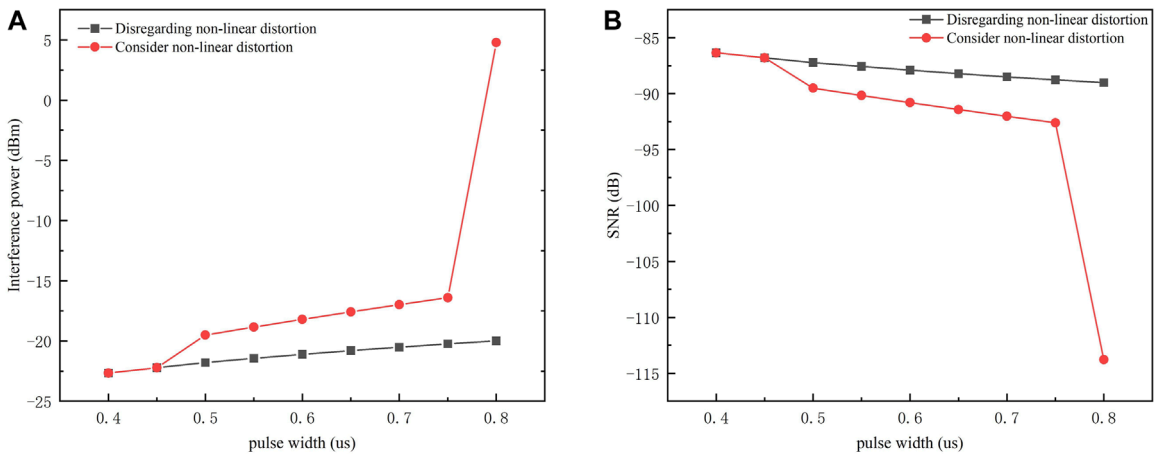

FIGURE 6
Variations in receiver interference power **(A)** signal-to-noise ratio **(B)**. As the pulse width increases, the interference power falling into the receiver gradually increases, and when it exceeds the input 1 dB compression point of the linear device, different linear devices successively produce nonlinear distortion, making the signal-to-trunk-noise ratio value change abruptly.

Upon integrating the data presented in Figure 6 below with that of Table 4 above, it is observable that with the increment of pulse width, the interference power encroaching upon the receiver's bandwidth gradually intensifies. Furthermore, when exceeding the input 1 dB compression point of the linear devices, nonlinear distortion is sequentially induced across various devices. This results in an abrupt alteration of the signal-to-carrier-to-noise ratio.

In an extensive review of the existing literature on electrothermal stress, scholars such as D.C. Wunsch, Jian-Guo Wang, and Liang Zhou [43] have conducted detailed evaluations of the damage mechanisms instigated by high-repetition-rate pulses on LNA devices. Their insightful analyses offer substantial theoretical validation for the distortion studies in LNAs, bolstering the understanding of LNA performance under stressed conditions.

Previously, in a seminal study conducted in 1998, T. Weissgerber delved into the effects of injected pulses on TTL logic gates and complementary metal-oxide-semiconductor (CMOS) circuits. It was concluded that with an increase in pulse frequency, there correspondingly was an escalation in the threshold power level required to maintain the tested device's functional integrity [44]. In a related vein, C.D. Taylor, in 1994, unveiled that the injection of high-power microwave signals spanning pulse widths from 100 nanoseconds to several microseconds, with field intensities fixed at 30 V/m, precipitated functional degradation or complete

failure within devices operating in the High Power Electromagnetic (HPEM) frequency band ranging from 0.2 to 5 GHz. Although it is recognized that high-power microwaves outside this frequency band are no less deleterious to system stability, scholarly endeavors have primarily centered on addressing concerns within the HPEM domain [45].

Building upon these foundational studies, D.C. Wunsch formulated what is now known as the Wunsch-Bell relationship. This refers to the association between a device's threshold power and the pulse bandwidth. The empirical relationship emerged from rigorous experimentation on the effects of high-power microwave radiation damage and has been corroborated by a series of subsequent experimental studies [46–49]. This relationship plays a crucial role in predicting the survivability of electronic components under high-energy pulses.

Furthering the quest for knowledge, in 2022, a research team helmed by Jian-Guo Wang at Xi'an Jiaotong University provided new insights into the phenomenon. The team documented that the threshold power for devices decreased precipitously with an increase in the pulse width for narrow pulses. However, as the pulse width reached a certain threshold, the decline in device threshold power plateaued, indicating a region of stability despite varying pulse parameters. It must be noted that due to the limitations of pulse source capabilities at the time, the vast majority of high-power microwave experiments reported in the literature employed pulse widths on the order of hundreds of nanoseconds up to the microsecond level, with typical repetition frequencies not exceeding 10 kHz [50].

Scholarly discourse has further expanded with contributions from researchers such as Tasca [51], who have engaged in comprehensive examinations of the intricate interdependence between device threshold power and the attributes of the introduced high-power signals. From an empirical stance, Benford [52] conducted experimental analyses revealing a noteworthy trend: the threshold power sufficient to inflict damage upon systems demonstrated a decrease coincident with the rise in system integration levels and the increment of clock frequencies. Through the synthesis of such extensive research endeavors, comprehensive literature reviews have encapsulated the diverse range of damage threshold powers observed across multiple systems under examination. These reviews have been integral in addressing the variations in susceptibility to damage arising from both direct and indirect pathways of high-power microwave interference.

In a significant advance within electronic device failure studies, Bo Zhang and his team at the University of Electronic Science and Technology of China presented a pivotal examination in 2022 [53]. Their comprehensive research shed light on the progressive deterioration of LDMOSFET devices, ascribing the root cause to the synergistic effects of gate trapping and consequent electrothermal stress amid a regime of repetitive pulse exposure. In the specific context of dual-trench LDMOSFETs, it was observed that subjecting the devices to a regimen of more than 1,200 V, delivered across 2,000 cycles, instigated the formation of a conspicuous crack within the gate oxide layer at its most indented region. This was proficiently identified via the employment of advanced electron microscopy techniques. Subsequent metrics revealed a quantifiable degradation, evidenced by a 5% reduction in on-resistance when juxtaposed with the parameters measured during lower power activities, before the onset of damage. Correspondingly, it was documented that the threshold damage power also underwent a 5% diminution. Comparatively, the asymmetric trench LDMOSFETs, upon enduring 12,000 pulses, presented a leakage current that escalated beyond the 10 mA threshold. Concurrently, there was a marked 10% increment in on-resistance relative to the pre-damage levels, whereas the threshold damage power exhibited a remarkable retention of its initial value.

In precursor studies during the years 2020 and 2021, Yan-Tang Yang et al. from Xidian University [9, 54] delved into the evaluation of variations in internal current density via simulations, as well as the behavior of charge carriers—in particular holes and electrons—in HEMT and CMOS devices under continuous high-power radiation. A significant finding emerged from these simulations of CMOS devices, illustrating a frequency-dependent shift in current type. It was ascertained that as the operational frequency was escalated from 1 to 3.5 GHz, the internal current transitioned from being predominantly electron-based to hole-based. Intriguingly, the densities of both carriers reached equilibrium at approximately 1.8 GHz.

Progressing the investigation into the realm of failure analysis under the influence of high-power microwaves, Liang Zhou [43] and his team have expanded the purview to encompass a broader spectrum of internal failure mechanisms beyond the thermal dimension. Their innovative work entailed crafting a series of high-power microwave injection experiments [52], aimed at scrutinizing the complex distribution of electrothermal stress fields within LNA devices confronting high-power pulses. The research meticulously addressed the interplay between threshold damage power and pulse width, alongside the consequences of thermal accumulation. Empirical validation was achieved as the computed stress field distributions displayed a robust congruity with the actual measured curves, thereby affirming the experimental analysis pioneered by their predecessors. This congruence not only reinforces the validity of the underlying models but also provides actionable insights into the intricate dynamics governing device reliability under such extreme conditions.

These mechanistic analysis results align with the theoretical experimental analysis of the impacts of high-repetition-rate pulse interference power on receiver distortion.

3.3 Filter response distortion

When high repetition frequency interference pulses enter the receiver, they bypass the limiter's clip-leak effect and are directly transmitted to the next stage without the limiter's influence. Since the third-order intermodulation distortion power generated by the low-noise amplifier and the mixer is much smaller than the power of the target echo signal, it is assumed that both are operating in an ideal state for further analysis.

Upon summarizing the experimental analysis of high-repetition-rate pulses interfering with the bandpass filter located after the limiter, it is concluded that empirical studies ([40–42], [55, 56]) consistently demonstrate that when the pulse width of an input repetition signal remains below the threshold of the receiver's response time, overlapping of interference signals manifests at both the leading and trailing edges of the filtered pulse. As the

signal travels through the detection process, this superposition acts perniciously, compromising the radar's ability to discern relevant signals. It has been inferred that such an eventuality results in the radar's inability to execute normal detection functions, with the interference signals effectively obfuscating the *bona fide* radar echo. This phenomenon reflects the critical nature of pulse width in relation to the response time of the radar system, illuminating the necessity for meticulous calibration of system parameters to ensure optimal performance.

It has been observed [5,6] that when the pulse width of the input signal surpasses the defined response time, the potential for adjacent pulse overlap becomes mitigated post the filtering of the interference pulse. However, it is the adjacent sidebands that then predominantly contribute to noise demodulation interference. Particularly under conditions where the interference power crosses a critical threshold, this form of interference gains prominence, exerting a suppression effect on the signal deemed effective. The findings suggest that the spatial interstice between pulses has a significant bearing on the extent of interference experienced by the system. Moreover, the data implies that while avoiding pulse overlap is beneficial, the power levels of interference within the adjacent sidebands must be closely monitored and controlled to prevent signal degradation and maintain the fidelity of the true signal within a navigator system's operational framework.

By simplifying the process in which high-repetition-rate pulses and effective signals enter the receiver, pass through the bandpass filter, and have the mixer directly shift the signal spectrum to the baseband, an analysis of the filter can be conducted. Experimental analysis [57] has shown that the high-repetition-rate pulses undergo bandwidth reduction, amplitude weakening, and pulse width broadening after being processed by the successive stages of filters in the receiver. Only a small portion of the interference energy can enter the subsequent pulse compression module of the receiver, thus affecting the detection of satellite signals.

4 Conclusion

Current interference analysis about high-repetition-rate pulses on navigation receivers generally investigates the receivers unlock conditions through theoretical analysis and simulation experiments. The study of the interference effects of high repetition frequency pulses is relatively mature. However, there is a scarcity of research on the mechanism analysis of the distortion in the front-end of the receiver caused by high repetition frequency pulse interference, with transient response and nonlinear distortion as the primary fields of study. In this paper, we encapsulate the mechanism analysis of the interference of interference on the front-end of the receiver.

From the review of the distortion types in the receiver and the signal processing flow, we summarized the transient response interference analysis of limiters and AGC, the nonlinear distortion interference analysis of LNA and mixers, and the distortion interference analysis on filter responses.

1. The analysis of the transient response mechanism showed that peak leakage significantly enhances nonlinear distortion, leading to higher input signal power to the Low Noise Amplifier (LNA) and exacerbating intermodulation distortion. When the received signal's power is beyond the receiver's dynamic range, it results in saturation and gain compression in the analog front end.
2. High-repetition-rate pulses extend interference signal duration and cause abnormal Automatic Gain Control (AGC) voltages, ultimately reducing gain. LNA and limiter respond nonlinearly, with the LNA exhibiting the most prolonged responses. Passive devices narrow the spectrum and elongate the temporal waveform, further affecting active component output duration.
3. Post-LNA processing of high-repetition-rate pulses can cause third-order intermodulation distortion, affecting subsequent signal processing stages. The mixer, particularly sensitive to non-linear distortion, especially at interference power levels beyond −20 dBm, becomes a critical point of concern. The threshold power of electronic devices like LNAs varies under pulse stress, and resilience is observed at certain pulse widths. High-power microwave radiation can cause progressive electrothermal damage in devices, suggesting the need for rigorous testing against both direct and indirect damage pathways.
4. For GNSS receivers, lower pulse repetition frequency (PRF) poses less interference unless the PRF harmonics fall within the operational bandwidth, with maximum interference occurring when PRF harmonics coincide with the GNSS signal's central frequency. Pulse width relative to response time also affects signal suppression and noise modulation, impacting effective signal detection when interference power is sufficiently large.

In terms of future directions, current research predominantly focuses on isolated analyses of individual modules. A promising avenue for advancement lies in conducting a comprehensive, full-pathway analysis of the receiver's RF front-end. This approach would entail a detailed examination of the cascading effects initiated by each module, thereby yielding a more holistic understanding of the underlying mechanisms. Furthermore, integrating this analysis with the signal processing modules of the receiver's backend, such as loop tracking, could offer a more nuanced and complete perspective on this field of study. Such multidimensional research would not only elucidate the impact mechanisms of high-repetition-rate pulses on GNSS receivers but also pave new pathways for the refinement of receiver hardware and signal processing techniques. Ultimately, this could provide a robust theoretical foundation for the development of receivers that are resilient to such interference in the future.

Author contributions

YS: Investigation, Writing–original draft, Writing–review and editing. HW: Data curation, Investigation, Project administration, Software, Writing–review and editing. WL: Methodology, Supervision, Writing–review and editing. WX: Conceptualization, Project administration, Supervision, Validation, Visualization,

Writing–review and editing. XY: Data curation, Formal Analysis, Project administration, Supervision, Validation, Writing–review and editing. GS: Conceptualization, Project administration, Resources, Software, Validation, Writing–review and editing.

Funding

The author(s) declare that financial support was received for the research, authorship, and/or publication of this article. This research was funded by National Key R&D Program of China, grant number 2023YFC2205400, the National Natural Science Foundation of China under grant number U20A0193, and the Hunan Provincial Science and Technology Innovation Program under grant number 2021RC3073.

Conflict of interest

The authors declare that the research was conducted in the absence of any commercial or financial relationships that could be construed as a potential conflict of interest.

Publisher's note

References

1. He H. *Research on anti-jamming technology for GNSS receivers*. China: University of Electronic Science and Technology (2013) PhD Thesis.

2. Issam S, Adnane A, Madiabdessalam A. Anti-Jamming techniques for aviation GNSS-based navigation systems: survey. In: *2020 IEEE 2nd international conference on electronics, control, optimization and computer science (ICECOCS)* (2020) 1–4. doi:10.1109/ICECOCS50124.2020.9314449

3. Qiang H, Sun L. Exploration of high repetition frequency pulse jamming technology. In: *Journal of Chinese academy of electronics and information technology* (2006) 147–51.

4. Zhao Y. "Research on radar jamming technology based on high repetition frequency ultra-wideband pulses." (2015) Master's Thesis.

5. Nan H, Wang X, Xu Z. Study on the interference mechanism of high repetition frequency pulses on the front end of passive guidance heads. *Mod Defense Technology* (2018) 46(82-87+158). doi:10.3969/j.issn.1009-086x.2018.05.13

6. Zhang Z, Jiang T, Cao R. High repetition frequency ultra-wideband short electromagnetic pulse interference on GPS receivers. *High Power Laser Part Beams* (2014) 26:177–82. doi:10.3788/HPLPB201426.033006

7. Uslenghi P, Erricolo D, Yang H-Y *Analysis and design of ultra wide-band and high-power microwave pulse interactions with electronic circuits and systems*, 55 (2007).

8. You H, Fan J, Jia X, Zhang L. Experimental research on the damage effect of HPM on semiconductor bipolar transistor. In: *2010 10th IEEE international conference on solid-state and integrated circuit technology* (2010) 1671–3. doi:10.1109/ICSICT.2010.5667381

9. Liu R, Ting L, Peng S. Impact of pulse interference on BeiDou B1I signal receivers. *Sci Technology Eng* (2020) 20:9062–8. doi:10.3969/j.issn.1671-1815.2020.22.031

10. Swami A, Sadler B, Turner J. On the coexistence of ultra-wideband and narrowband Radio systems. *2001 MILCOM Proc Commun Network-Centric Operations: Creating Inf Force (Cat. No.01CH37277)* (2001) 1:16–9. doi:10.1109/MILCOM.2001.985756

11. Earl GF. Receiving system linearity requirements for HF radar. *IEEE Trans Instrumentation Meas* (1991) 40(6):1038–41. doi:10.1109/19.119789

12. Wang J, Yuan Y. Nonlinear analysis and testing of receivers. *Syst Eng Electronics* (2003) 165–7. doi:10.3321/j.issn:1001-506X.2003.02.009

13. Nan H, Peng S, Wang G, Wang X. Interference mechanism of high repetition frequency pulses on guide head parameter sorting. *Radar Sci Technology* (2020) 1:102–8. doi:10.3969/j.issn.1672-2337.2020.01.017

14. Weibo X, Liu Z, Wang S, Shen T. Modeling study on the interference process of high repetition frequency laser on laser guidance heads. *Laser & Infrared* (2021) 1:29–33. doi:10.3969/j.issn.1001-5078.2021.01.005

15. Wang M. Mechanism research on high-power microwave repetitive pulse effects on PIN limiters. In: *Master's thesis, China academy of engineering physics* (2018).

16. Huang K, Wang B. Analysis of the response of high-power PIN diode limiter to the trailing edge of electromagnetic pulses. *High Power Laser Part Beams* (2008) 1177–81.

17. Yang J, Yang M, Meng Q, Zheng X. Application and development of ultra-wideband electromagnetic pulses in impulse radar. *Informatization Res* (2020) 1:8–12.

18. Chen Y, Zhili ZL, Yu H. Research on short recovery time technology for receiver protectors. *J Microwaves* (2023) 39(68-71+76). doi:10.14183/j.cnki.1005-6122.202301013

19. Fan Y, Zhang Q, Chen Y. Analysis of the destructive effects of high-power microwave bombs on GNSS receivers. *Syst Eng Electronics* (2020) 42(37–44). doi:10.3969/j.issn.1001-506X.2020.01.06

20. Wang H, Jiayin L, Li H, Yihong Z, Xiuyun Y. Transient response study of PIN limiters. In: *Proceedings of the 8th national laser science and technology youth academic exchange conference*. Fuzhou: University of Electronic Science and Technology of China (2005) 496–9.

21. Yong X, hua L, Hepeng fei, Qiu W. Estimating the interference of UWB pulse signal to GPS receiver. In: *2006 6th international conference on ITS telecommunications*. Chengdu, China: IEEE (2006) 286–9. doi:10.1109/ITST.2006.288875

22. Padgett JE, Koshy JC, Triolo AA. *Physical-layer modeling of UWB interference effects*. Fort Belvoir, VA: Defense Technical Information Center (2003) doi:10.21236/ADA525522

23. Morton YT, French MP, Zhou Q, Tsui JBY, Lin DM, Miller MM, et al. A software approach to access ultra-wide band interference on GPS receivers. *PLANS 2004* (2004) 551–7. Position Location and Navigation Symposium (IEEE Cat. No.04CH37556). doi:10.1109/PLANS.2004.1309041

24. Bangju H, Xiao S. Study on the interference of UWB communication signals to GPS receivers. *J Inf Eng Univ* (2006) 7(3):237–40. doi:10.3969/j.issn.1671-0673.2006.03.009

25. Tongcheng Z, Daojie Y, Dongfang Z, Mengjuan C, Kai H, Changlin Z, et al. Effects and experimental analysis of ultra-wideband electromagnetic pulses on UAV GPS receivers. *High Power Laser Part Beams* (2019) 31(2):45–9. doi:10.11884/HPLPB201931.180365

26. Huang X, Chen Y, Wang Y. Simulation of interference effects of UWB pulse signal to the GPS receiver. Editor S Wen (2021) 1–8. doi:10.1155/2021/9935543*Discrete Dyn Nat Soc*

27. Bhattacharya S, Senguttuvan R, Chatterjee A. Production test method for evaluating the effect of narrow-band interference on data errors in ultra-wide band (UWB) receivers. *IEEE MTT-S Int Microwave Symp Dig* (2005) 2005:1513–6. doi:10.1109/MWSYM.2005.1516981

28. Luo M, Akos D, Koenig M, Opshaug G, Pullen S, Enge P, et al. Testing and research on interference to GPS from UWB transmitters. (2001).

29. Zhang X, Song Q, Han Z, Zhang X. The simulation and analysis of the interference from ultra-wideband system to spread spectrum communication system. In: *2008 8th international symposium on antennas, propagation and EM theory*. China: IEEE: Kunming (2008) 1528–33. doi:10.1109/ISAPE.2008.4735523

30. Bin L. Application of high power microwave weapons in air defense. *Electron Sci Technology* (2011) Available from: https://api.semanticscholar.org/CorpusID:203977720. Accessed January 5, 2024.

31. Yuan H. Study on countermining GPS with high power microwave weapon (2008) Available from: https://api.semanticscholar.org/CorpusID:112464749. Accessed February 15, 2024.

32. Zhang Y-H, Huang W-H, Li P, Fang W-R, Zhang C-B. Interference mechanism of high repetitive frequency UWS-emp to communication receiver. In: *2017 IEEE 5th international Symposium on electromagnetic compatibility (EMC-Beijing), 1–5*. China: IEEE: Beijing (2017). doi:10.1109/EMC-B.2017.8260391

33. Yonglong L, Yuan X, Jiulong L, Zhengkun C, Zhiqiang D. Ground receiver interference technology of distributed ultra-wideband electromagnetic pulses based on low earth orbit satellites. *High Power Laser Part Beams*(2023) 3:81–7. doi:10.11884/HPLPB202335.220225

34. Xiao T, Wu Z, Liu C. The third-order intermodulation characteristics and experimental measurement of microwave power amplifiers. *Television Technology* (2019) 43(92–97). doi:10.16280/j.videoe.2019.02.020

35. Wang T, Peng S, Wang G. Analysis of the interference mechanism of high repetition frequency pulses on the front end of GPS receivers. *J Air Force Early Warning Acad* (2021) 35:248–53. doi:10.3969/j.issn.2095-5839.2021.04.004

37. Bradaric I, Capraro GT, Weiner DD. *Ultra wide band (UWB) interference - assessment and mitigation studies*. Fort Belvoir, VA: Defense Technical Information Center (2006) doi:10.21236/ADA446049

36. Jie X, Zhou W. Study on the interference of UWB signals to GPS. *Mod Electron Technology* (2005) 14–16. doi:10.3969/j.issn.1004-373X.2005.07.006

38. Anderson DSD. Assessment of compatibility between ultrawideband (UWB) systems and global positioning system (GPS) receivers (2001) Available from: https://bg.sunwayinfo.com.cn/report_detail?id=9ac511e5-3388-4ccf-a8ce-b828898c3617. Accessed January 4, 2024.

39. Lu T, Zhang H, Cui X, Gulliver TA. Power spectrum analysis of interference to a beidou satellite receiver from UWB impulse Radio sysems. In: *2014 12th international conference on signal processing (ICSP)*. Zhejiang, China: IEEE: Hangzhou (2014).1561–5. doi:10.1109/ICOSP.2014.7015260

40. Zhang K, Ouyang X, Yuan Z. Analysis of the suppression interference effects on GPS. *Commun Technology* (2018) 51:2544–8. doi:10.3969/j.issn.1002-0802.2018.11.003

41. Liu Y-Q, Chai C-C, Wu H, Zhang Y-H, Shi C-L, Yang Y-T. Mechanism of AlGaAs/InGaAs pHEMT nonlinear response under high-power microwave radiation. *IEEE J Electron Devices Soc* (2020) 8:731–7. doi:10.1109/JEDS.2020.3008816

42. Ding M, Feng Y, Dai W. Analysis of the impact of pulse interference on software receivers. *Navigation Positioning and Timing* (2017) 4(58–65). doi:10.19306/j.cnki.2095-8110.2017.03.010

43. Zhang Y, Liang Z. Failure and protection analysis of semiconductor devices under high-power microwave. *Saf Electromagn Compatibility* (2023) 6(December):9–20. doi:10.3969/j.issn.1005-9776.2023.06.001

44. Weissgerber T, Peier D, Hirsch H. Electromagnetic susceptibility of TTL and CMOS inverters. Influence of pulseform and external elements. *Proc 6th Int Conf Optimization Electr Electron Equipments* (1998) 1:257–62. doi:10.1109/OPTIM.1998.710484

45. Taylor CD, Giri DV. High power microwave systems and effects (1994) Available from: https://api.semanticscholar.org/CorpusID:106563934. Accessed February 5, 2024.

46. Wunsch DC, Bell RR. Determination of threshold failure levels of semiconductor diodes and transistors due to pulse voltages. *IEEE Trans Nucl Sci* (1968) 15(6):244–59. doi:10.1109/TNS.1968.4325054

47. Mansson D, Thottappillil R, Backstrom M, Lunden O. Vulnerability of European rail traffic management system to radiated intentional EMI. *IEEE Trans Electromagn Compatibility* (2008) 50(1):101–9. doi:10.1109/TEMC.2007.915281

48. Fang J, Liu G, Ping L, Wang H, Huang W. Experimental study on the effects of high-power microwave pulse width. *High Power Laser Part Beams* (1999) 11(5):639–42.

49. Guo H, Hui Z, Chen Y, Zhang Y, Gong R, Ying G, et al. Two-dimensional numerical simulation of the failure and burnout of PN junctions caused by fast-rising edge electromagnetic pulses with different rise times. *Microelectronics Comput* (2002) 19(3):17–20. doi:10.3969/j.issn.1000-7180.2002.03.005

50. Li Y, Xie H, Yan H, Wang J, Yang Z. A thermal failure model for MOSFETs under repetitive electromagnetic pulses. *IEEE Access* (2020) 8:228245–54. doi:10.1109/ACCESS.2020.3045621

51. Wen Y, Xinhua C, Huang W, Liu G. The relationship between diode failure and burnout threshold and electromagnetic wave parameters. *High Power Laser Part Beams* (2000) 12(2):215–8.

52. Serafin DJ, Dupouy DD. Potential iemi threats against civilian air traffic. (2005).

53. Deng X, Huang W, Li X, Li X, Chen C, Wen Y, et al. Investigation of failure mechanisms of 1200 V rated trench SiC MOSFETs under repetitive avalanche stress. *IEEE Trans Power Electronics* (2022) 37(9):10562–71. doi:10.1109/TPEL.2022.3163930

54. Liang Q-S, Chai C-C, Wu H, Liu Y-Q, Fu-Xing L, Yang Y-T. Mechanism analysis and thermal damage prediction of high-power microwave radiated CMOS circuits. *IEEE Trans Device Mater Reliability* (2021) 21(3):444–51. doi:10.1109/TDMR.2021.3104760

55. Chen T. Design and implementation of GPS targeted jamming device. In: *Master's thesis*. Harbin, China: Harbin Engineering University (2016).

57. Karbolin VA, Nosov VI, Kalinin VO. Performance analysis of UWB communication receiver in multipath environment based on RAKE receiver. In: *2020 21st international conference of young specialists on micro/nanotechnologies and electron devices (EDM)*. IEEE: Chemal, Russia (2020) 98–103. doi:10.1109/EDM49804.2020.9153501

56. Quincy EA. Victim receiver response to ultrawideband signals. *2001 MILCOM Proc Commun Network-Centric Operations: Creating Inf Force (Cat. No.01CH37277)* (2001) 1:20–4. doi:10.1109/MILCOM.2001.985757